Sub-barrier fusion of ^{32}S+^{90,96}Zr: semi-classical coupled-channels approach

H. Q. Zhang[1], C. J. Lin[1], F. Yang[1], H. M. Jia[1], X. X. Xu[1], F. Jia[1],
Z. D. Wu[1], S. T. Zhang[1], Z. H. Liu[1], A. Richard[1,2,3], and C. Beck[2]

[1]*China Institute of Atomic Energy, P. O. Box 275(10),*
Beijing 102413, P. R. China
[2]*Institut Pluridisciplinaire Hubert Curien, UMR 7178,*
CNRS-IN2P3, and Université de Strasbourg (UdS),
F-67037 Strasbourg Cedex 2, France
[3]*Ecole Nationale Supérieure de Physique de Strasbourg (ENSPS),*
F-67400 Illkirch, France

(Dated: May 6, 2010)

The fusion excitation functions have been measured with rather good accuracy for ^{32}S+^{90}Zr and ^{32}S+^{96}Zr near and below the Coulomb barrier. The sub-barrier cross sections for ^{32}S+^{96}Zr are much larger compared with ^{32}S+^{90}Zr. Semi-classical coupled-channels calculations including two-phonon excitations are capable to describe sub-barrier enhancement only for ^{32}S+^{90}Zr. The remaining disagreement for ^{32}S+^{96}Zr comes from the positive Q-value intermediate neutron transfers in this system. The comparison with ^{40}Ca+^{96}Zr suggests that couplings to the positive Q-value neutron transfer channels may play a role in the sub-barrier fusion enhancement. A rather simple model calculation taking neutron transfers into account is proposed to overcome the discrepancies of ^{32}S+^{96}Zr.

PACS numbers: 25.70.Gh, 25.70.Jj, 24.10.Eq

I. INTRODUCTION

The heavy-ion fusion reactions in the low-energy range near and below the Coulomb barrier have been the subject of extensive experimental and theoretical efforts in the past decades [1–3]. Beside the fact that the questions of the possible occurence of unexpected phenomena, such as breakup effects on the fusion reactions at near barrier energies [3], are still unresolved, one has still to understand better the role of neutron transfers in the fusion process [4, 5]. For instance, effects of neutron-rich projectiles on the formation of superheavy elements (SHE) [6], especially with the development of newly available Radioactive Ion Beams (RIB) facilities need to be clarified as well as fusion hindrance at extremely low energies that remain among the most interesting open questions in the nuclear astrophysics domain [7]. Fusion enhancement below the Coulomb barrier is one of the most studied phenomena and, measurements of fusion barrier distributions have been widely performed to investigate the mutual importance of both the nuclear structure and dynamical process effects on the sub-barrier fusion enhancement [8–14].

Coupled-channels (CC) calculations have been used to describe the reactions in this energy range theoretically (see for example Refs. [1, 8] and references therein). Fusion enhancement due to the static deformations and surface vibrations of the nuclei has been well described in the coupled-channels calculations [8–14].

The influence of the neutron transfer channels on sub-barrier fusion process [11–17] is not yet fully understood. During the last 20 years a large number of experimental and theoretical investigations were undertaken to study the neutron-transfer mechanisms in competition with the fusion process. Stelson *et al*. [15–17] proposed an original scenario that uses an empirical method involving a sequential transfer of several neutrons between the reactants. This multineutron transfer process is capable to initiate fusion at large internuclear distances and will smooth the fusion barrier distributions (with larger width) with lower energy thresholds. This "shift" effect corresponds to the energy window for which the nuclei are allowed to come sufficiently close together for neutrons to flow freely between the target and projectile. As a consequence, this will reduce the effective barrier and enhance the fusion cross sections at sub-barrier energies. Following this idea, Rowley *et al*. [18] have first used a simple phenomenological model that simulates coupling to neutron transfer channels with a parametrized coupling matrix. Later on, Zagrebaev [19] proposed another semiclassical theoretical model that has been successfully used to reproduce the sub-barrier fusion enhancement of the old ^{40}Ca+^{96}Zr reaction data of Ref. [11] by including the intermediate positive Q-value neutron transfer channels in the CC calculations.

The failure of the CC calculations including only the couplings to the inelastic excitations indicates that couplings to neutron transfer channels may play a key role in the fusion dynamics near the barrier for medium-heavy systems such as ^{40}Ca+^{90,96}Zr [11, 20], ^{36}S+^{90,96}Zr [21], and ^{20}Ne+^{90,92}Zr [22], the last two reactions being studied by measurements of large-angle quasielastic scattering. Previous measurement of quasielastic scatterings of ^{32}S+^{90,96}Zr were also undertaken at backward angles near the barrier [23]; their analysis gave indication that positive Q-value neutron transfer channels should be included in the coupling scheme. Up to now no fusion data exist neither for ^{20}Ne+^{90,92}Zr nor for the ^{32}S+^{90,96}Zr reactions, it will be interesting to measure their fusion excitation functions. In order to disentangle the possible effect of positive Q-value neutron transfer couplings we decided to investigate the two last systems. We report here about the measurement of near- and sub-barrier fusion

excitation functions of ^{32}S+^{90}Zr and ^{32}S+^{96}Zr performed with small energy steps and good statistics accuracy.

Our research will focus on the role of neutron transfers between the colliding nuclei as a mechanism that enhances the fusion cross sections at sub-barrier energies. This paper is organized as follows: Sec. II presents the experimental setup and details on the measurements. Results of the analysis of the experimental data are given in Sec. III. Their discussion is finally proposed in Sec. IV in the framework of comparisons with semiclassical coupled-channels calculations before a short summary of the Sec. V.

II. EXPERIMENTAL PROCEDURES

The experiment was performed at the HI-13 tandem accelerator of CIAE, Beijing. The collimated ^{32}S (Q = 10$^+$ charge state) beam was used to bombard the zirconium oxide targets. The beam intensity was stabilized in the 2-20 pnA range in order to minimize the pile-up for each of the bombarding energies. The 3 mm diameter (98.87% enriched) ^{90}ZrO$_2$ and (86.4% enriched) ^{96}ZrO$_2$ targets were both 50 μg/cm^2 thick and evaporated onto 15 μg/cm^2 carbon foil backings. The beam energies varied over the range E_{lab} = 100-130 MeV for ^{32}S+^{90}Zr and E_{lab} = 95-130 MeV for ^{32}S+^{96}Zr (in 1.33 Mev steps at the higher and 0.67 MeV at the lower energies) and changed only downwards starting at E_{lab} = 130 MeV in order to reduce the magnetic hysteresis for both targets. The target chamber contains four silicon detectors at θ = ±25 ° symmetrically (right/left and up/down) with respect to the beam axis in the forward direction in order to monitor the beam optics (Rutherford scattering) and to provide an absolute normalization of the fusion cross sections.

The fused evaporation residues (ER) concentrated to within a few degrees of the incident beam direction were separated from the incident beam (see Fig. 1) by an electrostatic deflector which design is pretty much similar to the experimental setup in Legnaro [24]. It consists of two pairs of electrodes followed by an E-TOF arrangement with of a microchannel plate (MCP) detector coupled to a Si(Au) surface barrier detector. Two-dimensional plots of the data were used to cleanly separate the ER's from the beam-like products (BLP). A typical example of the time-of-flight versus energy spectrum for ^{32}S+^{96}Zr measured at E_{lab} = 130 MeV and θ = 2 ° is shown in Fig. 1. The electrostatic deflector could be rotated about the target position in the horizontal plane to measure the ER angular distributions.

The particles coming from the target were selected before entering the fields by an entrance collimator of 3 mm diameter, corresponding to a $\Delta\theta$ = ± 0.57 ° opening. A 10μg/cm^2 thick carbon foil clung to the collimator was used to reset the atomic charge state distribution on the ion path. The collimator of the MCP defined the solid angle of the electrostatic deflector as being approximately $\Delta\Omega$ = 0.3 msr.

ER angular distributions were measured in the range θ = -4 ° to θ = 10 ° with step $\Delta\theta$ = 1 ° at three beam energies (E_{lab} = 100, 115, and 130 MeV) for both systems. The angular dis-
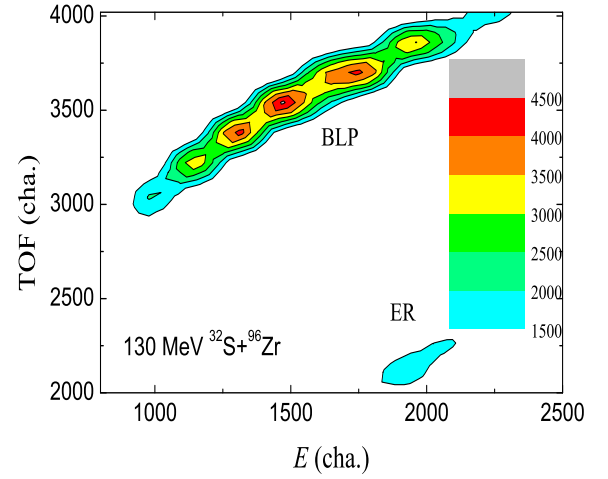

FIG. 1: (Color online) Two-dimensional plot E-TOF of the events, following beam separation, taken at E_{lab} = 130 MeV and at 2 ° for the ^{32}S+^{96}Zr reaction. Two groups of particles [beam-like particles(BLP) and evaporation residues (ER)] are indicated.

tributions were found to be symmetrical about θ = 0 °, as expected. Their typical shape did not change appreciably with the beam energy. These combined angular distributions and the double Gaussian fits were used to obtain the fusion cross sections. At each energy the number of ER events was normalized to the Rutherford scattering rates counted by the monitor detectors. For the most of energy points, only differential cross sections were measured at θ = 2 °, from the obtained values, the total ER cross sections were deduced. Using the solid angles, the θ = 2 °-to-total ratios and the measured transmission efficiencies, these ER yields were transformed into total cross sections. Since fission of the compound nucleus can be neglected for both systems, the measured cross sections were taken as complete fusion cross section σ_f.

The transmission efficiencies and the relevant voltages used to deflect the ER were calibrated by the ^{122}Ba beam scattered by the ^{90}Zr target at small angles and at the corresponding energies with the fusion evaporation residues. It was found that the defocusing effect of the deflection voltage reduces the transmission from unity to 0.60±0.06. Additional systematic errors come from the geometrical solid angle uncertainties, the angular distribution integrations, and the transmission measurements. Altogether these contributions sum up to a ± 15% value for systematic errors.
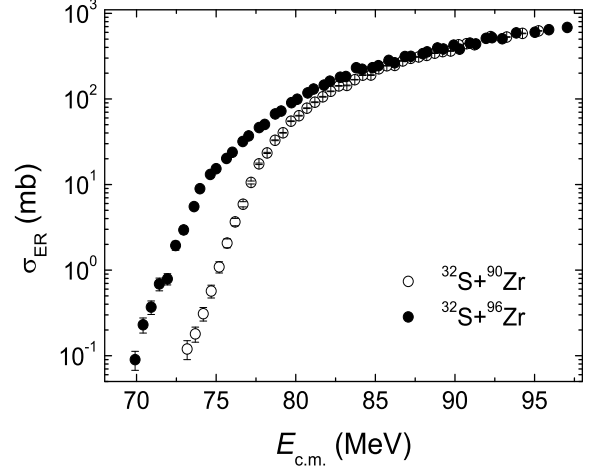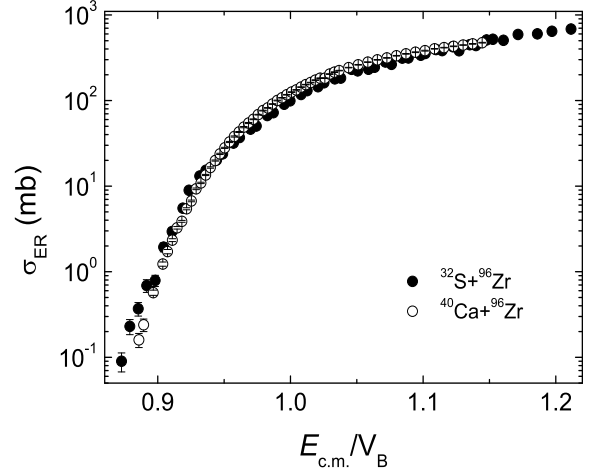
III. EXPERIMENTAL RESULTS

The measured ER excitation functions for the two systems are shown in Fig. 2, where the energy scale is corrected for the target thickness. The statistical errors shown in the figure do not exceed the symbol size for most of the experimental points. They are ± 0.8% for both the high-energy and the intermediate-energy points and increase to ± 23% for the low-energy points. The ER cross sections are listed in Tables I and II for both reactions.

TABLE I: Experimental ER cross sections for ^{32}S+^{90}Zr.

$E_{c.m.}$ (MeV)	σ_{ER} (mb)	$E_{c.m.}$ (MeV)	σ_{ER} (mb)
95.3	623.51±4.00	82.7	142.10±1.37
94.2	582.98±4.63	82.2	122.84±1.08
93.3	528.80±3.93	81.7	105.94±1.10
92.2	535.48±4.70	81.2	91.59±0.92
91.2	430.00±3.37	80.7	77.96±0.80
90.7	442.29±3.03	80.2	63.69±0.62
90.2	429.44±3.58	79.7	54.96±0.55
89.7	363.05±3.22	79.2	40.22±0.39
89.2	357.17±2.84	78.7	32.89±0.34
88.7	342.70±2.94	78.2	23.41±0.35
88.2	322.27±3.07	77.7	17.46±0.35
87.7	309.41±2.80	77.2	10.58±0.42
87.2	298.07±2.85	76.7	5.89±0.41
86.7	277.99±2.29	76.2	3.66±0.37
86.2	246.27±2.81	75.7	2.07±0.25
85.7	244.09±2.02	75.2	1.09±0.16
85.2	224.93±1.95	74.7	0.57±0.10
84.7	190.06±1.64	74.2	0.31±0.06
84.2	189.70±1.75	73.7	0.18±0.04
83.7	167.85±1.25	73.2	0.12±0.03
83.2	143.85±1.38		

TABLE II: Experimental ER cross sections for ^{32}S+^{96}Zr.

$E_{c.m.}$ (MeV)	σ_{ER} (mb)	$E_{c.m.}$ (MeV)	σ_{ER} (mb)
97.1	683.96±3.93	82.1	161.35±1.34
95.9	644.56±7.76	81.8	145.06±1.51
95.0	601.59±3.70	81.1	130.62±1.09
93.9	591.22±4.33	80.8	117.57±1.21
93.0	505.50±3.00	80.1	99.28±0.85
92.3	519.80±4.10	79.7	90.53±0.83
92.0	510.25±3.57	79.1	72.13±0.66
91.3	439.19±3.38	78.7	66.85±0.70
90.9	448.78±3.14	78.1	50.41±0.43
90.3	381.53±2.95	77.7	46.28±0.51
89.9	424.93±3.13	77.0	37.01±0.31
89.3	382.96±3.02	76.7	31.81±0.34
88.9	393.91±2.55	76.0	23.82±0.03
88.3	354.74±2.11	75.7	20.18±0.03
88.0	338.00±2.74	75.0	15.32±0.23
87.2	314.40±2.44	74.6	13.12±0.26
86.9	313.05±2.37	74.0	8.95±0.36
86.2	264.38±2.37	73.6	5.53±0.39
85.8	282.11±2.51	73.0	2.95±0.30
85.2	244.76±1.78	72.5	1.94±0.23
84.8	231.95±2.18	71.9	0.79±0.12
84.2	222.32±1.83	71.4	0.69±0.12
83.8	231.63±1.93	70.9	0.37±0.07
83.2	182.87±1.85	70.4	0.23±0.05
82.8	179.30±1.82	69.9	0.09±0.02

FIG. 2: Experimental ER excitation functions of ^{32}S+^{90}Zr (hollow circles) and ^{32}S+^{96}Zr (solid circles) as a function of the center-of-mass energy. The error bars represent purely statistical uncertainties.

FIG. 3: Plot of the ER excitation functions on a reduced-energy scale for the two systems ^{32}S+^{96}Zr (filled circles) measured in the present work and ^{40}Ca+^{96}Zr (open circles). The data for ^{40}Ca+^{96}Zr are taken from Ref. [11].

The comparison of the ER excitation functions of ^{32}S+^{96}Zr (present work) and ^{40}Ca+^{96}Zr [11] is made easier when cross sections are plotted in a reduced-energy scale as shown in Fig. 3. One observes that the two systems display very similar behaviors on the whole energy range despite relatively large discrepancies. These discrepancies are mainly due to larger uncertainties in the present data arising from larger backgrounds in the spectra. It is interesting to notice that both system reactants have very similar nuclear structures as well as neutron-transfer properties. This behavior, already discussed in our previous investigation of ^{32}S+^{90,96}Zr quasielastic barrier distributions [23], indicates that the positive Q-value neutron transfers strongly enhance the fusion cross sections at sub-barrier energies. This experimental observation will be confirmed by the semiclassical coupled-channels calculations as
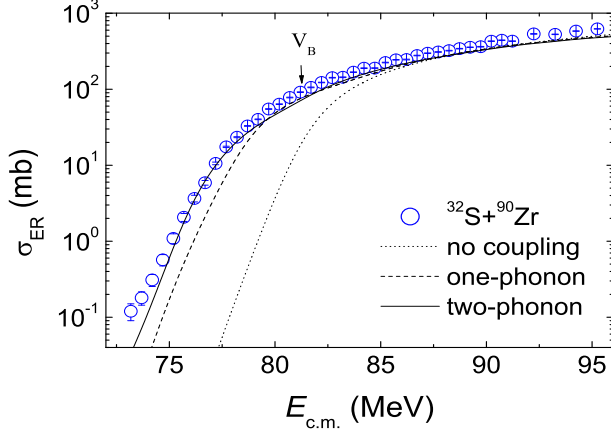
FIG. 4: ER excitation function of ^{32}S+^{90}Zr. The open circles are the experimental data. The dotted, dashed, and solid lines represent the CCFULL calculations without coupling and with the one-phonon and two-phonon couplings, respectively (see text for details). The arrow indicates the position of the Coulomb barrier for ^{32}S+^{90}Zr.

FIG. 5: ER excitation functions of ^{32}S+^{96}Zr. The solid circles are the experimental data. The dotted, dashed and dash-point lines are the CCFULL calculations with no coupling, one-phonon and two-phonon couplings, respectively. The solid line is the calculation taking into account the neutron transfers by NTFus code. The arrow indicates the position of the Coulomb barrier for ^{32}S+^{96}Zr.

discussed in the following Section.

IV. DISCUSSION: SEMICLASSICAL COUPLED-CHANNELS CALCULATIONS

The ER excitation functions of ^{32}S+^{90}Zr and ^{32}S+^{96}Zr have been compared with the results of CC calculations performed with the CCFULL code [26] using the Akyüz-Winther nuclear potential [27].

The relevant informations on the low-lying excitations of ^{32}S, ^{90}Zr, and ^{96}Zr can be seen in Table III. The quadrupole vibrations of both ^{90}Zr and ^{96}Zr nuclei are weak in energy: in fact, they lie at comparable energies. With this potential the CCFULL barriers were found to be at V$_B$ = 81.2 MeV for ^{32}S+^{90}Zr and at V$_B$ = 80.1 MeV for ^{32}S+^{96}Zr, respectively. These values are fully consistent with what was found for the quasielastic barriers previously measured by our group [23]. In a first approximation, these values can be considered as average values between the barrier heights for the nose-to-nose configuration and for the side-to-side configuration [25].

Figures 4 and 5 show the comparisons of the experimental ER excitation functions and the CCFULL calculations with one- and two-phonon couplings and without coupling for the ^{32}S+^{90,96}Zr fusion reactions. Semiclassical coupled-channels calculations have also been performed by use of the new code NTFus [28] where the proximity potential is adopted. The new oriented object code has been constructed in the framework of the Zagrebaev model [25] and implemented in C^{++} by using the compiler of ROOT [29]. More technical details and related discussions about the NTFus code will be illustrated elsewhere [28].

First we propose to present the calculations for ^{32}S+^{90}Zr that are displayed in Fig. 4. They were performed without taking the neutron transfers into account. The two-phonon coupling CCFULL calculations are quite satisfactory. The
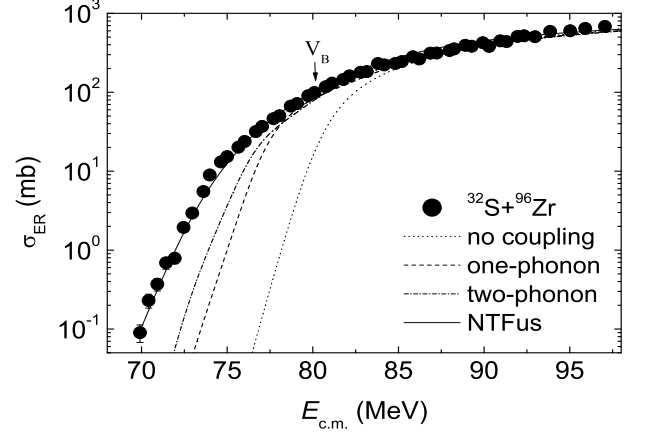
calculation (solid line) reproduces the data below and above the barrier V$_B$ (arrow in Fig.4). On the other hand, the calculations fail for ^{32}S+^{96}Zr with large discrepancies occuring mainly at energies below the barrier V$_B$ (arrow in Fig.5). One- and two-phonon (both shown in Fig. 5) excitations in ^{96}Zr, of both quadrupole and octupole natures, bring additional but not sufficient enhancements. Finally, we tried also "three-phonon" couplings, but no further improvement could be reached. Anyway, additional couplings in ^{32}S+^{96}Zr, which might give rise to lower-energy barriers, are simply not present in the coupling scheme. Similar conclusions have been obtained for the ^{40}Ca+^{94}Zr reaction [14].

When we choose to take into account the neutron transfers, the fusion excitation function can be derived using the following formula [19]:

$$T_l(E) = \int f(B) \frac{1}{N_{tr}} \sum_k \int_{-E}^{Q_0(k)} \alpha_k(E, l, Q)$$
$$\times P_{HW}(B, E + Q, l) dQ dB, \qquad (1)$$

and

$$\sigma_{fus}(E) = \frac{\pi \hbar^2}{2\mu E} \sum_{l=0}^{l_{cr}} (2l + 1) T_l(E), \qquad (2)$$

where $T_l(E)$ is the transmission, E the energy at the center-of-mass, $f(B)$ the normalized barrier distribution function, l the momentum and l_{cr} the critical momentum calculated where there is no coupling (well above the barrier). $\alpha_k(E,l,Q)$ and $Q_0(k)$ are the probability and the Q-value for the transfer of k neutrons, $1/N_{tr}$ is the normalization of the total probability taking into account the neutron transfers.

The calculation with the neutron transfer effect is performed up to the channel +4n (k=4). No more visible effect

TABLE III: Excitation energies E_x, spin and parities λ^π, and deformation parameters β_λ for ^{32}S and ^{90,96}Zr.

Nucleus	E_x (MeV)	λ^π	β_λ
^{32}S	2.230	2^+	0.32
	5.006	3^-	0.40
^{90}Zr	2.186	2^+	0.09
	2.748	3^-	0.22
^{96}Zr	1.751	2^+	0.08
	1.897	3^-	0.27

TABLE IV: Q-value in MeV for neutron pickup transfer channels from ground state to ground state for the ^{32}S+^{90,96}Zr systems.

System	+1n	+2n	+3n	+4n
^{32}S+^{90}Zr	-3.33	-1.229	-6.59)	-6.319
^{32}S+^{96}Zr	0.788	5.737	4.508	7.655

can be obtained by using +5n and +6n channels. More details of the calculation procedures and of the description of the NTFus code [28], itself, will be given in a forthcoming Brief Report. The Q-values for the calculation (solid line in Fig. 5) are given in Table IV. As we can see in Fig. 5, the dash-point line (without the neutron transfers) does not at all describe the data at the sub-barrier energies. In contrast, the solid line taking into account the neutron transfers is able to fit the data reasonably well. As expected, the correction applied on the calculation at sub-barrier energies by the Zagrebaev model [19, 25] enhances the cross sections further. Moreover, it allows a fairly good description of the present experimental data showing the strong effect of neutron transfers for the sub-barrier fusion of ^{32}S+^{96}Zr.

Figures 6 and 7 show the experimental barrier distributions from fusion and quasi-elastic scattering and the corresponding CCFULL calculations for the two systems. The fusion barrier distributions for the two systems have been obtained by double differentiation $E\sigma_{\mathrm{fus}}$ vs energy using the three-point difference formula [11]. The quasi-elastic barrier distributions are taken from Ref. [23]. It is very interesting to note that for both reactions the experimental quasi-elastic barrier distributions and the experimental fusion barrier distributions are strikingly similar. The large fluctuations occurs in the barrier distributions for $E_{\mathrm{c.m.}} > 80$ MeV is not enough due to the measuring accuracy of the ER cross sections. For ^{32}S+^{90}Zr, the overall trends of the experimental barrier distributions are roughly consistent with the CCFULL calculation considering the two-phonon coupling. While for ^{32}S+^{96}Zr, the experimental barrier distributions are wide and show a low-energy tail extending to the lowest energies compared with ^{32}S+^{90}Zr and the CCFULL calculation considering the two-phonon coupling. It shows a part loss of the component below 75 MeV. This is due to the coupling to the $Q > 0$ neutron transfers, corresponding to the further fusion enhancement at sub-barrier energies compared with the calculation.
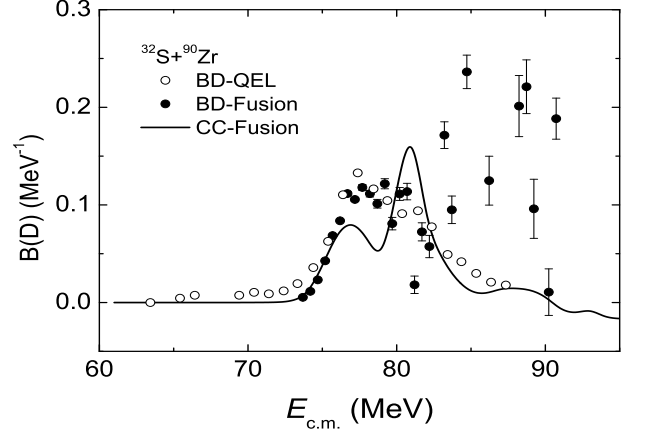

FIG. 6: Barrier distributions for ^{32}S+^{90}Zr from fusion (solid circles) and quasi-elastic scattering (hollow circles). The line is the CCFULL calculation with two-phonon coupling.
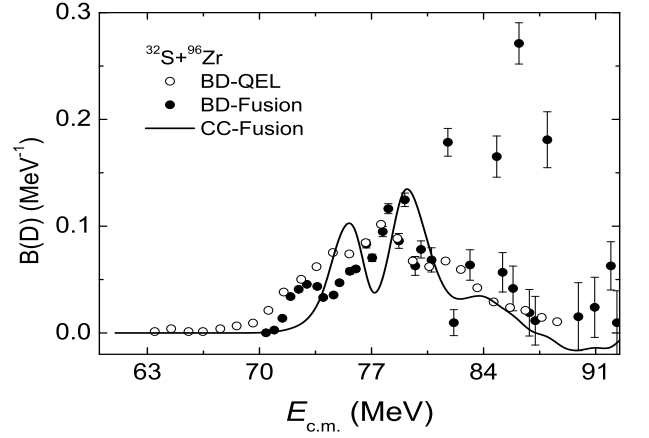

FIG. 7: For ^{32}S+^{96}Zr, the symbols are the same as in Fig. 6.

V. SUMMARY

The fusion excitation functions for ^{32}S+^{90,96}Zr were measured with a high precision near and below the Coulomb barrier. The sub-barrier cross sections for ^{32}S+^{96}Zr are much larger compared with ^{32}S+^{90}Zr. The data have been analyzed with both the CCFULL code and the NTFus code based on a semi-classical coupled-channels model, which includes the sequential neutron transfers for ^{32}S+^{96}Zr as earlier proposed by Zagrebaev. Good agreement between experimental data and the calculation is achieved for ^{32}S+^{90}Zr by including the couplings to the low-lying quadruple and octupole vibrations in ^{32}S and ^{90}Zr. Whereas the NTFus calculations can reproduce the data by including four sequential neutron transfer channels as well as the low-lying quadrupole and octupole vibrations in ^{32}S and ^{96}Zr. The comparison with previous data on ^{40}Ca+^{96}Zr shows that the excitation functions of ^{32}S, ^{40}Ca+^{96}Zr are very similar in the whole energy range. Both systems have similar collective states and positive Q-value neutron transfer channels. This comparison strongly supports

the previous suggestion [23] that positive Q-value neutron transfer channels enhance sub-barrier fusion cross sections, particularly at very low energies. Also the fusion and quasi-elastic barrier distributions of the ^{32}S+^{90,96}Zr systems are basically consistent in both cases. The two barrier distributions for ^{32}S+^{96}Zr cannot be reproduced by CCFULL code below 75 MeV. The fact shows again the effect of the $Q > 0$ neutron transfers on the sub-barrier fusion process. In addition to the fusion excitation function, the neutron transfer cross section measurement for this system should provide useful information on the coupling strength of neutron transfer channels, which will allow us to reach a much deeper understanding of the role of neutron transfer mechanisms, sequential or simultaneous, in the fusion process.

[1] A.B. Balantekin and N. Takigawa, Rev. Mod. Phys. **70**, 77 (1998).

[2] M. Dasgupta, D.J. Hinde, N. Rowley, and A.M. Stefanini, Annu. Rev. Nucl. Part. Sci. **48**, 401 (1998).

[3] L.F. Canto, P.R.S. Gomes, R. Donangelo, and M.S. Hussein, Phys. Rep. **424**, 1 (2006).

[4] R.A. Broglia, C.H. Dasso, S. Landowne, and A. Winther, Phys. Rev. C **27**, 2433 (1983).

[5] S.Y. Lee, Phys. Rev. C **29**, 1932 (1984).

[6] V.I. Zagrebaev, V.V. Samarin, and W. Greiner, Phys. Rev. C **75**, 035809 (2007).

[7] M.S. Smith and K.E. Rehm, Annu. Rev. Nucl. Part. Sci. **51**, 91 (2001).

[8] N. Rowley, G.R. Stachler, and P.H. Stelson, Phys. Lett. **B254**, 25 (1991).

[9] J.X. Wei, J.R. Leigh, D.J. Hinde, J.O. Newton, R.C. Lemmon, S. Elfstrom, J.X. Chen, and N. Rowley, Phys. Rev. Lett **67**, 3368 (1991).

[10] A.M. Stefanini, D. Ackermann, L. Corradi, D.R. Napoli, C. Petrache, P. Spolaore, P. Bednarczyk, H.Q. Zhang, S. Beghini, G. Montagnoli, L. Mueller, F. Scarlassara, G.F. Segato, F. Soramel, and N. Rowley, Phys. Rev. Lett **74**, 864 (1995).

[11] H.Timmers, D. Ackermann, S. Beghini, L. Corradi, J.H. He, G. Montagnoli, F. Scarlassara, A.M. Stefanini, and N. Rowley, Nucl. Phys. **A633**, 421 (1998).

[12] M. Trotta, A. M. Stefanini, L. Corradi, A. Gadea, F. Scarlassara, S. Beghini, and G. Montagnoli, Phys. Rev. C **65**, 011601(R) (2001).

[13] A.M. Stefanini, F. Scarlassara, S. Beghini, G. Montagnoli, R. Silvestri, M. Trotta, B.R. Behera, L. Corradi, E. Fioretto, A. Gadea, Y.W. Wu, S. Szilner, H.Q. Zhang, Z.H. Liu, M. Ruan, F. Yang, and N. Rowley, Phys. Rev. C **73**, 034606 (2006).

[14] A.M. Stefanini, B.R. Behera, S. Beghini, L. Corradi, E. Fioretto, A. Gadea, G. Montagnoli, N. Rowley, F. Scarlassara, S. Szilner, and M. Trotta, Phys. Rev. C **76**, 014610 (2007).

[15] P.H. Stelson, Phys. Lett. **B205**, 190 (1988).

[16] P.H. Stelson, H.J. Kim, M. Beckerman, D. Shapira, and R.L. Robinson, Phys. Rev. C **41**, 1584 (1990).

[17] D. Shapira, and P.H. Stelson, Phys. Rev. C **47**, 1666 (1993).

[18] N. Rowley, I.J. Thompson, and M.A. Nagarajan, Phys. Lett. **B282**, 276 (1992).

[19] V. I. Zagrebaev, Phys. Rev. C **67**, 061601(R) (2003).

[20] G. Montagnoli, S. Beghini, F. Scalassara, A.M. Stefanini, L. Corradi, C.J. Lin, G. Pollarolo, and Aage Winther, Eur. Phys. G. A **15**, 351 (2002).

[21] A.M. Stefanini, L. Corradi, A.M. Vinodkumar, Y. Feng, F. Scarlassara, G. Montagnoli, S. Beghini, and M. Bisogno, Phys. Rev. C 62, 014601 (2000).

[22] E. Piasecki, Ł. Świderski, W. Gawlikowicz, J. Jastrzębski, N. Keeley, M. Kisieliński, S. Kliczewski, A. Kordyasz, M. Kowalczyk, S. Khlebnikov, E. Koshchiy, E. Kozulin, T. Krogulski, T. Loktev, M. Mutterer, K. Piasecki, A. Piórkowska, K. Rusek, A. Staudt, M. Sillanpää, S. Smirnov, I. Strojek, G. Tiourin, W. H. Trzaska, A. Trzcińska, K. Hagino, and N. Rowley, Phys. Rev. C **80**, 054613 (2009).

[23] F. Yang, C.J. Lin, X.K. Wu, H.Q. Zhang, C.L. Zhang, P. Zhou, and Z.H. Liu, Phys. Rev. C **77**, 014601 (2008).

[24] S. Beghini, C. Signorini, S. Lunardi, M. Morando, G. Fortuna, A. M. Stefanini, W. Meczynski, and R. Pengo, Nucl. Instrum. Methods A **239**, 585 (1985).

[25] V. I. Zagrebaev, and V. V. Samarin, Phys. Atomic Nuclei **67**, 1462 (2004).

[26] K. Hagino, N. Rowley, and A.T. Kruppa, Comput. Phys. Commun. **123**, 143 (1999).

[27] Ö. Akyüz and A. Winther, in *Nuclear Structure and Heavy-Ion Reactions*, Proceedings of the International School of Physics "Enrico Fermi," Course LXXVII, Varenna, edited by R. A. Broglia *et al*. (North-Holland, Amsterdam, 1981).

[28] A. Richard, H.Q. Zhang, F. Yang, and C. Beck, submitted for publication.

[29] http://root.cern.ch, website of ROOT